On Intriguing Layer-Wise Properties of Robust Overfitting in Adversarial Training

Anonymous authors
Paper under double-blind review

Abstract

Adversarial training has proven to be one of the most effective methods to defend against adversarial attacks. Nevertheless, robust overfitting is a common obstacle in adversarial training of deep networks. There is a common belief that the features learned by different network layers have different properties, however, existing works generally investigate robust overfitting by considering a DNN as a single unit and hence the impact of different network layers on robust overfitting remains unclear. In this work, we divide a DNN into a series of layers and investigate the effect of different network layers on robust overfitting. We find that different layers exhibit distinct properties towards robust overfitting, and in particular, robust overfitting is mostly related to the optimization of latter parts of the network. Based upon the observed effect, we propose a *robust adversarial training* (RAT) prototype: in a minibatch, we optimize the front parts of the network as usual, and adopt additional measures to regularize the optimization of the latter parts. Based on the prototype, we designed two realizations of RAT, and extensive experiments demonstrate that RAT can eliminate robust overfitting and boost adversarial robustness over the standard adversarial training.

1 Introduction

Deep neural networks (DNNs) have been widely applied in multiple fields, such as computer vision (He et al., 2016) and natural language processing (Devlin et al., 2018). Despite its achieved success, recent studies show that DNNs are vulnerable to adversarial examples. Well-constructed perturbations on the input images that are imperceptible to human's eyes can make DNNs lead to a completely different prediction (Szegedy et al., 2013). The security concern due to this weakness of DNNs has led to various works in the study of improving DNNs robustness against adversarial examples. Across existing defense techniques thus far, Adversarial Training (AT) (Goodfellow et al., 2014; Madry et al., 2017), which optimizes DNNs with adversarially perturbed data instead of natural data, is the most effective approach (Athalye et al., 2018). However, it has been shown that networks trained by AT technique do not generalize well (Rice et al., 2020). After a certain point in AT, immediately after the first learning rate decay, the robust test accuracy continues to decrease with further training. Typical regularization practices to mitigate overfitting such as l1 & l2 regularization, weight decay, data augmentation, etc. are reported to be as inefficient compared to simple early stopping (Rice et al., 2020).

Many studies have attempted to improve the robust generalization gap in AT, and most have generally investigated robust overfitting by considering DNNs as whole. However, DNNs trained on natural images exhibit a common phenomenon: features obtained in the first layers appear to be general and applicable widespread, while features computed by the last layers are dependent on a particular dataset and task (Yosinski et al., 2014). Such behavior of DNNs sparks a question: Do different layers contribute differently to robust overfitting? Intuitively, robust overfitting acts as an unexpected optimization state in adversarial training, and its occurrence may be closely related to the entire network. Nevertheless, the unique effect of different network layers on robust overfitting is still unclear. Without a detailed understanding of the layer-wise mechanism of robust overfitting, it is difficult to completely demystify the exact underlying cause of the robust overfitting phenomenon.

In this paper, we provide the first layer-wise diagnosis of robust overfitting. Specifically, instead of considering the network as a whole, we treat the network as a composition of layers and systematically investigate the impact of robust overfitting phenomenon on different layers. To do this, we first fix the parameters for the selected layers, leaving them unoptimized during AT, and then normally optimize other layer parameters. We discovered that robust overfitting is always *mitigated* in the case where the latter layers are left unoptimized, and applying the same effect to other layers is *futile* for robust overfitting, suggesting a strong connection between the optimization of the latter layers and the overfitting phenomenon.

Based upon the observed effect, we propose a *robust adversarial training* (RAT) prototype to relieve the issue of robust overfitting. Specifically, RAT works in each mini-batch: it optimizes the front layers as usual, and for the latter layers, it implements additional measures on these parameters to regularize their optimization. It is a general adversarial training prototype, where the front and latter network layers can be separated by some simple test experiments, and the implementation of additional measures to regularize network layer optimization can be versatile. For instance, we designed two representative methods for the realizations of RAT: RAT_{LR} and RAT_{WP}. They adopt different strategies to hinder weight update, e.g., enlarging the learning rate and weight perturbation, respectively. Extensive experiments show that the proposed RAT prototype effectively eliminates robust overfitting. The contributions of this work are summarized as follows:

- We provide the first diagnosis of robust overfitting on different network layers, and find that there is a strong connection between the optimization of the latter layers and the robust overfitting phenomenon.
- Based on the observed properties of robust overfitting, we propose the RAT prototype, which adopts additional measures to regularize the optimization of the latter layers and is tailored to prevent robust overfitting.
- We design two different realizations of RAT, with extensive experiments on a number of standard benchmarks, verifying its effectiveness.

2 Related Work

2.1 Adversarial Training

Since the discovery of adversarial examples, there have been many defensive methods attempted to improve the DNN's robustness against such adversaries, such as adversarial training (Madry et al., 2017), defense distillation (Papernot et al., 2016), input denoising (Liao et al., 2018), gradient regularization (Tramèr et al., 2018). So far, adversarial training (Madry et al., 2017) has proven to be the most effective method. Adversarial training comprises two optimization problems: the inner maximization and outer minimization. The first one constructs adversarial examples by maximizing the loss and the second updates the weight by minimizing the loss on adversarial data:

$$\ell^{\text{AT}}(\boldsymbol{w}) = \min_{w} \sum_{i} \max_{d(x_i, x_i') \leq \epsilon} \ell(f_w(x_i'), y_i), \tag{1}$$

where f_w is the DNN classifier with weight w, and $\ell(\cdot)$ is the loss function. $d(.,.)$ specify the distance between original input data x_i and adversarial data x_i', which is usually an l_p-norm ball such as the l_2 and l_∞-norm balls and ϵ is the maximum perturbation allowed.

A different type of AT variation that is commonly used is referred to as TRADES (Zhang et al., 2019), which involves optimizing a surrogate loss that is a tradeoff between the natural accuracy and adversarial robustness:

$$\ell^{\text{TRADES}}(\boldsymbol{w}) = \min_{w} \sum_{i} \left\{ \text{CE}(f_w(x_i), y_i) \quad + \beta \cdot \max_{d(x_i, x_i') \leq \epsilon} \text{KL}(f_w(x_i) || f_w(x_i')) \right\}, \tag{2}$$

The surrogate loss consists of two parts: cross-entropy (CE) loss, which encourages the network to maximize natural accuracy, and Kullback-Leibler (KL) divergence, which encourages the improvement of robust accuracy. The hyperparameter β is used to control the tradeoff between natural accuracy and adversarial robustness.

2.2 Semi-supervised learning

Another line of work involves utilizing semi-supervised learning (SSL) technique. Methods based on SSL use additional unlabeled data to improve the robustness of the trained model. In these methods, a natural model is first trained on labeled data to generate pseudo-labels for the unlabeled data. Then, a robust model is trained using an adversarial loss function $\ell(\boldsymbol{w})$ on both labeled and unlabeled data:

$$\ell^{\text{SSL}}(\boldsymbol{w}) = \ell^{\text{labeled}}(\boldsymbol{w}) + \lambda \cdot \ell^{\text{unlabeled}}(\boldsymbol{w}), \tag{3}$$

where λ control the weight on the unlabeled data. We introduces some notable works surrounding semi-supervised learning below:

- Najafi et al. (2019) examine the robust semi-supervised learning approach using distributionally robust optimization. Their method involves assigning soft labels to unlabeled data based on an adversarial loss and training such images with labeled ones. Their experiments demonstrate that the proposed algorithm enhances adversarially robust generalization across a variety of tasks.
- Uesato et al. (2019) investigate the robustness of a Gaussian mixture model proposed by Schmidt et al. (2018) and demonstrate that a self-training approach can effectively utilize unlabeled data to improve the model's adversarial robustness. They apply the self-training algorithm on the real-world image dataset CIFAR-10, combined with unlabeled Tiny Image dataset, and achieve state-of-the-art adversarial robustness. Their approach shows significant improvements in low-labeled data regimes by removing most of the labels from CIFAR-10 and SVHN datasets.
- Carmon et al. (2019) achieve comparable theoretical and empirical outcomes as (Uesato et al., 2019), while also providing a more comprehensive examination of additional facets. They demonstrate that by leveraging unlabeled data and robust self-training, the trained models can achieve enhanced certified robustness against all potential attacks. Additionally, they investigate the effects of various training components on the ultimate model performance, including the size of the unlabeled data.
- Zhai et al. (2019) leverage risk decomposition theorem by separating the expected robust risk into two components: stability and accuracy. The stability component measures the prediction stability in the presence of perturbations, and the accuracy component measures the standard classification accuracy. As the stability component does not require label information, it can be optimized using unlabeled data. Their study focuses on a specific Gaussian mixture problem inspired by Schmidt et al. (2018), which shows that adversarial robust generalization can be almost as easy as standard generalization in supervised learning if a sufficiently large amount of unlabeled data is provided.

2.3 Robust generalization

An interesting characteristic of deep neutral networks (DNNs) is their ability to generalize well in practice (Belkin et al., 2019). For the standard training setting, it is observed that test loss continues to decrease for long periods of training (Nakkiran et al., 2020), thus the common practice is to train DNNs for as long as possible. However, in the case of adversarial training, further training past a certain point leads to a significant decrease in the robust training loss of the classifier, while increasing the robust test loss. Figure 1 depicts this phenomenon for adversarial training on CIFAR-10, where the robust test accuracy initially increases but then drops after the first learning rate decay. This phenomenon is called "robust overfitting", which has shown strong resistance to standard regularization techniques such as l_1, l_2 regularization and data augmentation methods, and can be observed on various datasets, including SVHN, CIFAR-100, and ImageNet (Rice et al., 2020).

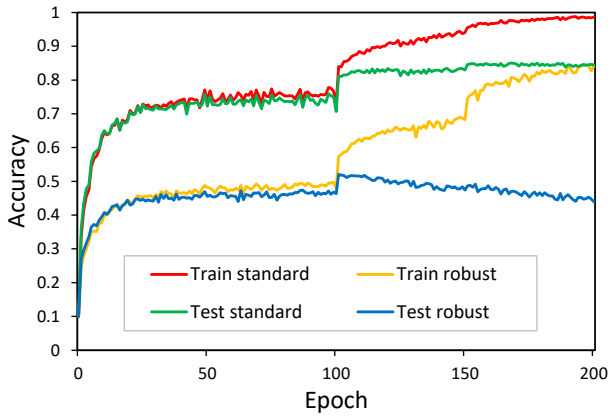

Figure 1: The learning curves of adversarial training using PreAct ResNet-18 on the CIFAR-10 dataset. The depicted curves reveal "robust overfitting", wherein the adversarially trained model briefly achieves 52.01% test robust accuracy shortly after the first learning rate decay. Surprisingly, at this point, the adversarially trained model is actually more robust than it is at the end of training, where it only attains a 43.95% test robust accuracy against a 20-step PGD adversary with an ℓ_∞ radius of $\epsilon = 8/255$. The learning rate is decayed at 100 and 150 epochs.

Schmidt et al. (2018) theorizes that robust generalization have a large sample complexity, which requires substantially larger dataset. Many subsequent works have empirically validated such claim, such as AT with semi-supervised learning (Carmon et al., 2019; Zhai et al., 2019), robust local feature (Song et al., 2020) and data interpolation (Lee et al., 2020; Chen et al., 2021a). Chen et al. (2020) proposes to combine smoothing the logits via self-training and smoothing the weight via stochastic weight averaging to mitigate robust overfitting. Wu et al. (2020) emphasizes the connection of weight loss landscape and robust generalization gap, and suggests injecting the adversarial perturbations into both inputs and weights during AT to regularize the flatness of weight loss landscape. The intriguing property of robust overfitting has motivated great amount of study and investigation (Wang et al., 2019; Zhang et al., 2020; Liu et al., 2021; Rebuffi et al., 2021; Dong et al., 2022b; Yu et al., 2022; Dong et al., 2022a; Li & Spratling, 2023; Wang et al., 2023), but current works typically approach the phenomenon considering a DNN as a whole. In contrast, our work treats a DNN as a series of layers and reveals a strong connection between robust overfitting and the optimization of the latter layers, providing a novel perspective into better understanding the phenomenon.

3 Intriguing Properties of Robust Overfitting

In this section, we first investigate the layer-wise properties of robust overfitting by fixing model parameters in AT (Section 3.1). Based on our observations, we further propose a robust adversarial training (RAT) prototype to mitigate robust overfitting (Section 3.2). Finally, we design two different realizations for RAT to verify the effectiveness of the proposed method (Section 3.3).

3.1 Layer-wise Analysis of Robust Overfitting

Current works usually study the robust overfitting phenomenon considering the network as a single unit (Rice et al., 2020; Wu et al., 2020; Yu et al., 2022; Dong et al., 2022a; Li & Spratling, 2023; Wang et al., 2023). However, features computed by different layers exhibit different properties, such as first-layer features are general and last-layer features are specific (Yosinski et al., 2014). We hypothesize that different network layers have different effects on robust overfitting. To empirically verify the above hypothesis, we deliberately fix the parameters of the selected network layers, leaving them unoptimized during AT and observe the behavior of robust overfitting accordingly. Specifically, we considered PreAct ResNet-18 architecture as a composition of 4 main layers, corresponding to 4 Residual blocks. We then train multiple PreAct ResNet-18

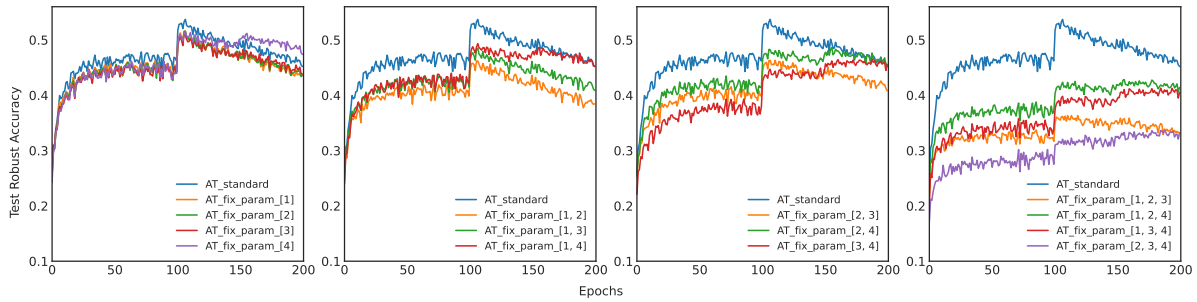

(a) Robust test performance

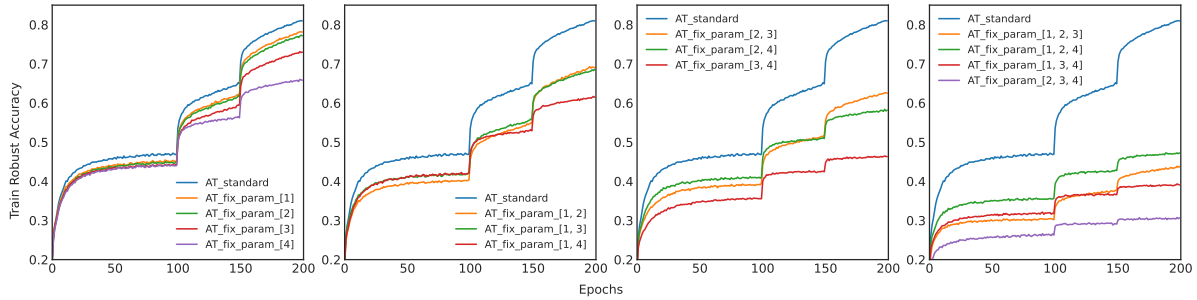

(b) Robust train performance

Figure 2: The robust train/test performance of adversarial training with different sets of network layers fixed. AT-fix-param[1,2] corresponds to fixing the parameters of layers 1 & 2 during AT.

networks on CIFAR-10 for 200 epochs using AT, each time selecting a set of network layers to have their parameter fixed.

The robust test performance in Figure 2(a) shows a consistent pattern. Robust overfitting is mitigated whenever we fix the parameters for layer 4 during AT, while any settings that do not fix the parameters for layer 4 result in a more severe gap between the best accuracy and the accuracy at the last epoch. For example, for settings such as AT-fix-param-[4], AT-fix-param-[1,4], AT-fix-param-[2,4] and AT-fix-param-[3,4], robust overfitting is significantly reduced. On the other hand, for settings such AT-fix-param-[1,2], AT-fix-param-[1,3] and AT-fix-param-[2,3], when we fix the parameters of various set of layers but allow for the optimization of layer 4, robust overfitting still widely exists. For extreme case like AT-fix-param-[1,2,3], where we fix the first three front layers and only allow for the optimization of that last layer 4, the gap between the best accuracy and the last accuracy is still obvious. This clearly indicates that the optimization of the latter layers present a strong correlation to the robust overfitting phenomenon. Note that this relationship can be observed across a variety of datasets, network architectures, AT methods, and threat models (shown in Appendix A), indicating that it is a general property in adversarial training.

In many of these settings, robust overfitting is mitigated at the cost of robust accuracy. For example in AT-fix-param-[3,4], if we leave both layer 3 & 4 unoptimized, robust overfitting will practically disappear, but the peak performance is much worse compared to standard AT. When carefully examining the training performance in these settings shown in Figure 2(b), we generally observe that the network capacity to fit adversarial data is strong when we fix the parameters for the front layers, but it gradually gets weaker as we try to fix the latter layers. For instance, AT-fix-param-[1] has the highest train robust accuracy, then comes AT-fix-param[2], AT-fix-param[3] and AT-fix-param[4]; AT-fix-param[1,2,3] has higher training accuracy than AT-fix-param[2,3,4]. This suggests fixing the latter layers' parameters can regularize the network better compared to fixing the front layers's parameters. In the subsequent sections, we will introduce methods that specifically regularize the optimization of the latter layers, so as to mitigate robust overfitting without tradeoffs in robustness. We will compare the impact on robust overfitting when applied such methods on the

front layers vs the latter layers, further highlighting the importance of the latter layers in relation to robust overfitting.

3.2 A Prototype of RAT

As witnessed in Section 3.1, the optimization of AT in the latter layers is highly correlated to the existence of robust overfitting. To address this, we propose to train the network on adversarial data with some restrictions put onto the optimization of the latter layers, dubbed as *Robust Adversarial Training* (RAT). RAT adopts additional measures to regularize the optimization of the latter layers and mitigate robust overfitting.

The RAT prototype is given in Algorithm 1. It runs as follows. We start with a base adversarial training algorithm $\mathcal{A}$. In Line 1-3, The inner maximization pass aims to generate adversarial examples via maximizing the loss, and then the outer minimization pass updates the weight to minimize the loss on adversarial data. Line 4 initiates a loop through all parts of the weight w from the front layers to the latter layers. Line 5-9 then manipulate different parts of the weight based on its layer conditions. If the parts of the weight belong to the front layers ($\mathfrak{C}_{\text{front}}$), their gradients will be kept intact. Otherwise, a weight update scheme $\mathfrak{S}$ is put onto the parts of the weight corresponding to the latter layers ($\mathfrak{C}_{\text{latter}}$). Finally, the optimizer $\mathfrak{O}$ updates the model f_w in Line 11.

Note that RAT is a general prototype where layer conditions $\mathfrak{C}_{\text{front}}$, $\mathfrak{C}_{\text{latter}}$ and weight adjustment strategy $\mathfrak{S}$ can be versatile. For example, based on the observations in Section 3.1, we treat the ResNet architecture as a composition of 4 main layers, corresponding to 4 residual blocks, where $\mathfrak{C}_{\text{front}}$ indicates layer 1 & 2 and $\mathfrak{C}_{\text{latter}}$ indicates layer 3 & 4. $\mathfrak{S}$ can also represent various strategies that serves to regularize the optimization of the latter layers. In the section below, we will propose two different strategies $\mathfrak{S}$ in the implementations of RAT to demonstrate RAT's effectiveness.

Algorithm 1 RAT-prototype (in a mini-batch).

Require: base adversarial training algorithm $\mathcal{A}$, optimizer $\mathfrak{O}$, network f_w, model parameter $w = \{w_1, w_2, ..., w_n\}$, training data $\mathcal{D} = \{(x_i, y_i)\}$, mini-batch $\mathcal{B}$, front and latter layer conditions $\mathfrak{C}_{\text{front}}$ and $\mathfrak{C}_{\text{latter}}$ for f_w, gradient adjustment strategy $\mathfrak{S}$

1: Sample a mini-batch $\mathcal{B} = \{(x_i, y_i)\}$ from $\mathcal{D}$
2: $\mathcal{B}' = \mathcal{A}$.inner_maximization$(f_w, \mathcal{B})$
3: $\nabla_w \leftarrow \mathcal{A}$.outer_minimization$(f_w, \ell_{\mathcal{B}'})$
4: **for** $j = 1, ..., n$ **do**
5: **if** $\mathfrak{C}_{\text{front}}(w_j)$ **then**
6: $\nabla_{w_j} \leftarrow \nabla_{w_j}$
7: **else if** $\mathfrak{C}_{\text{latter}}(w_j)$ **then**
8: $\nabla_{w_j} \leftarrow \mathfrak{S}(f_w, \mathcal{B}', \nabla_{w_j})$ # adjust gradient
9: **end if**
10: **end for**
11: $\mathfrak{O}$.step(∇_w)

3.3 Two Realizations of RAT

In this section, we will propose two different methods to put certain restrictions on the optimization of selected parts of the network, and then investigate the robust overfitting behavior upon applying such method to the front layers vs the latter layers. These methods showcase a clear relation between the optimization of the latter layers and robust generalization gap.

RAT through enlarging learning rate. In standard AT, the sudden increases in robust test performance appears to be closely related to the drops in the scheduled learning rate decay. We hypothesize that training AT without learning rate decays is sub-optimal, which can regularize the learning process of adversarial training. Comparison of the train/test performance between standard AT and AT without learning rate decay (AT-fix-lr-[1,2,3,4]) are shown in Figure 3(b). Training performance of standard AT accelerates quickly right after the first learning rate drop, expanding the generalization gap with further training, whereas for

AT without learning rate decay, training performance increases slowly and maintain a stable generalization gap. This suggests that AT optimized without learning rate decay has less capacity to fit adversarial data, and thus provides the regularization needed to relieve robust overfitting. As our previous analysis suggests that the optimization of the latter layers is more important in mitigating robust overfitting, we propose using a fixed learning rate of 0.1 for optimizing the latter parts of the network while applying the piecewise decay learning rate for the former parts to close the robust generalization gap. We refer to this approach as a realization of RAT through enlarging learning rate, namely RAT_{LR}. Note that there is no difference between enlarging learning rate and enlarging gradients, since the amplification coeffcient has the same effects in increasing gradients and increasing the learning rate inside $\mathfrak{O}$. Therefore, compared to standard AT, RAT_{LR} essentially enlarge the weight gradient ∇_{w_j} along the latter layers by 10 at the first learning rate decay and 100 at the second decay:

$$\nabla_{w_j} = \eta \nabla_{w_j}, \tag{4}$$

where η is the amplification coefficient.

To demonstrate the effectiveness of RAT_{LR}, we train multiple PreAct ResNet-18 networks on CIFAR-10 for 200 epochs using AT, each time selecting a set of network layers to have their learning rate fixed to 0.1 while maintaining the piece-wise learning rate schedule for other layers. Figure 3(a) validate our proposition. Robust overfitting is relieved for all settings that target layers that include layer 4 (AT-fix-lr-[4], AT-fix-lr-[1,4], AT-fix-lr-[2,4], etc.) while any settings that fix the learning rate of layers that exclude layer 4 do not reduce robust overfitting. Furthermore, all settings that fix the learning rate for both layer 3 & 4, including AT-fix-lr-[3,4], AT-fix-lr-[1,3,4], AT-fix-lr-[2,3,4] & AT-fix-lr-[1,2,3,4] completely eliminate robust overfitting. The observations indicate that regularizing the optimization of the latter layers by optimizing those layers without learning rate decays can prevent robust overfitting from occurring. An important observation is that RAT_{LR} (AT-fix-lr-[3,4]) can both overcome robust overfitting and achieve better robust test performance compared to the network using a fixed learning rate for all layers (AT-fix-lr-[1,2,3,4]). Examining the training performance between these two settings in Figure 3(c), we find that RAT_{LR} exhibits a rapid rise in both robust and standard training performance immediately after the first learning rate decay similar to standard AT. The training performance of RAT_{LR} is able to benefit from the learning rate decay occurring at layer 1 & 2, making a notable improvement compared to AT-fix-lr-[1,2,3,4]. By training layers 3 & 4 without learning rate decays, we specifically put some restrictions on the optimization of only the latter parts of the network heavily responsible for robust overfitting, which can relieve robust overfitting without sacrificing too much performance. The experiment results provide another indication that the latter layers have stronger connections to robust overfitting than the front layers do, and regularizing the optimization of the latter layers from the perspective of learning rate can effectively mitigate robust overfitting.

RAT through adversarial weight pertubation. We continue to study the impact of different network layers to robust overfitting phenomenon from the perspective of adversarial weight perturbation (AWP). Wu et al. (2020) proposes AWP as a method to explicitly flatten weight loss landscape, by introducing adversarial perturbations into both inputs and weights during AT:

$$\min_{w} \max_{v \in V} \sum_{i} \max_{d(x_i, x_i') \leq \epsilon} \ell(f_{w+v}(x_i'), y_i), \tag{5}$$

where V is a feasible region for the perturbation v, and v is the adversarial weight perturbation generated by maximizing the classification loss:

$$v = \nabla_w \sum_i \ell_i, \tag{6}$$

where ℓ_i is the adversarial loss of x_i'. Then the norm of weight perturbation v_j is restricted by its relative size to the norm of model weight w_j:

$$||v_j|| = \gamma ||w_j||, \tag{7}$$

where γ is the constraint on weight perturbation size.

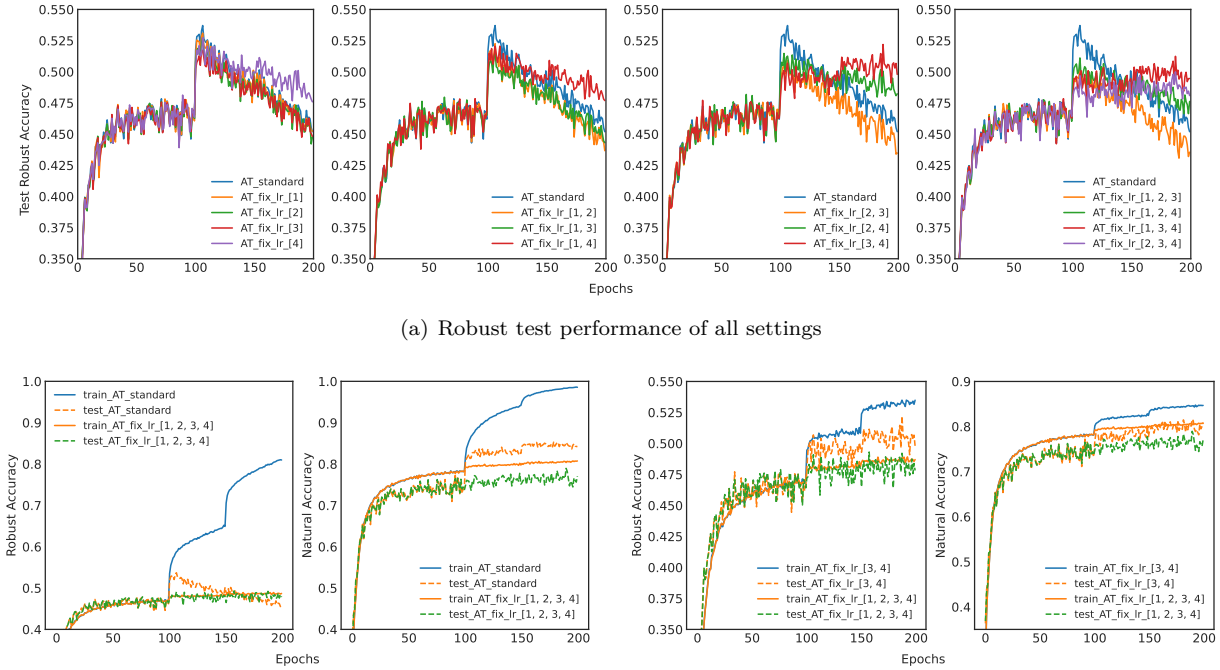

(a) Robust test performance of all settings

(b) Standard AT vs AT using a fixed learning rate

(c) AT using a fixed learning rate for all layers vs the latter layers

Figure 3: The train/test performance of adversarial training using a fixed learning rate for different sets of network layers. AT-fix-lr[1,2] corresponds to using a fixed learning rate for layers 1 & 2 during AT.

As AWP keeps injecting the worst-case perturbations on weight during training, it could also be viewed as a means to regularize the optimization of AT. In fact, the training of AWP exhibits a negative robust generalization gap, where robust training accuracy is in short of robust testing accuracy by a large margin, shown in Figure 4(c). This indicates AWP put significant restrictions to the optimization of AT, introducing huge trade-offs to training performance. As our previous analysis suggests a strong correlation between robust overfitting and the optimization of the latter layers, we argue that the capacity to mitigate robust overfitting from AWP is mostly thanks to the perturbations occurring at latter layers' weight. As such, we propose to specifically apply AWP to the latter half of the network, and refer to this method as RAT_{WP}. In essence, RAT_{WP} compute the adversarial weight perturbation v_j under the layer condition $\mathfrak{C}_{\text{latter}}(w_j)$, so that only the parts of the weight along the latter half of the network are perturbed:

$$\min_{\boldsymbol{w}=[w_1,\ldots,w_j,\ldots,w_n]} \max_{\boldsymbol{v}=[0,\ldots,v_j,\ldots 0]\in V} \sum_i \max_{d(x_i,x_i')\leq\epsilon} \ell(f_{\boldsymbol{w}+\boldsymbol{v}}(x_i'), y_i), \tag{8}$$

$$v_j = \nabla_{w_j} \sum_i \ell_i. \tag{9}$$

$$||v_j|| = \gamma ||w_j||. \tag{10}$$

To prove the effectiveness of RAT_{WP}, we train multiple PreAct ResNet-18 networks on CIFAR-10 for 200 epochs using AT, each time selecting a set of network layers to have their weight locally perturbed using AWP. As seen from Figure 4(a), there are only 3 settings that can overcome robust overfitting, namely AT-awp-[3,4], AT-awp-[1,3,4] and AT-awp-[2,3,4]. These settings share one key similarity: both layer 3 & 4 have their weight adversarially perturbed during AT. Simply applying AWP to any set of layers that exclude layers 3 & 4 is not sufficient to mitigate robust overfitting. This shows that AWP is effective in solving robust overfitting only when applied to both layer 3 and layer 4. Even when AWP is applied to the first 3 former layers out of 4 layers (AT-awp-[1,2,3]), robust overfitting still widely exists. In another word, it is essential

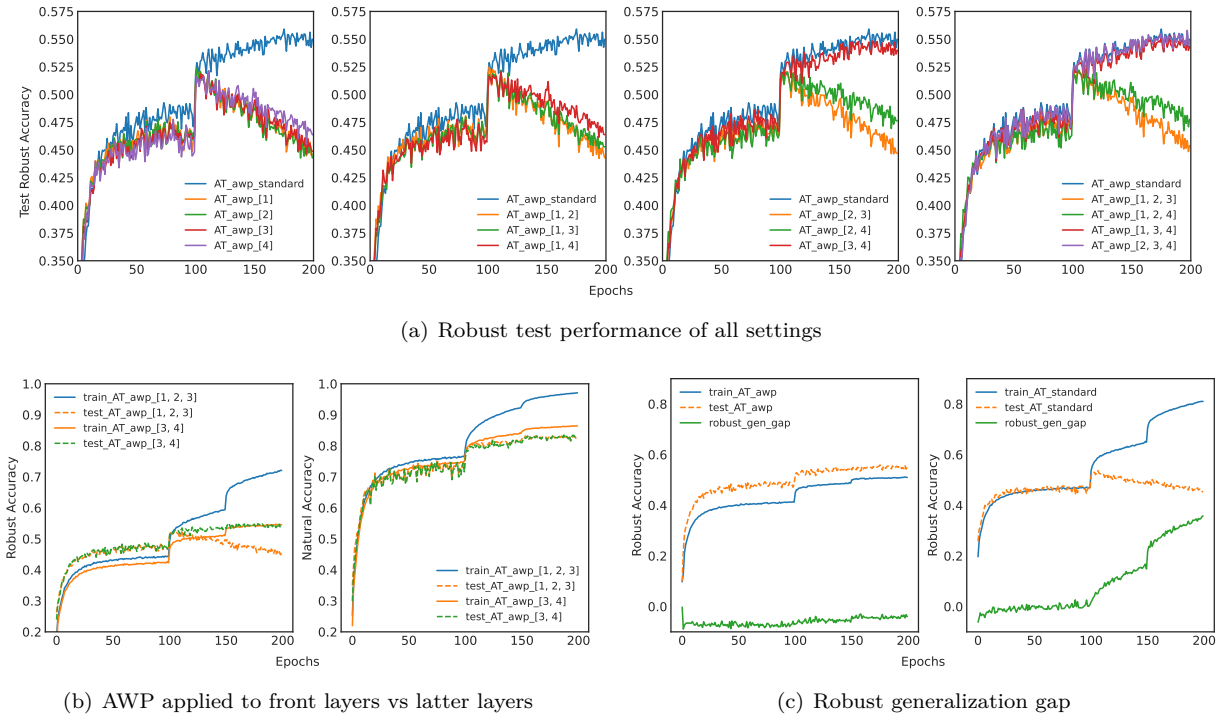

(a) Robust test performance of all settings

(b) AWP applied to front layers vs latter layers

(c) Robust generalization gap

Figure 4: The train/test performance of adversarial training when applying AWP for different sets of network layers. AT-awp-[1,2] means only layer 1 & 2 have their weight perturbed using AWP.

for the adversarial weight perturbations to occur at the latter part of the network in order to mitigate robust overfitting. To examine this phenomenon in detail, we compare the training performance of AWP applied to front layers (represented by AT-awp-[1,2,3]) vs AWP applied to latter layers (represented by AT-awp-[3,4]), shown in Figure 4(b). AWP applied in the front layers have a much better training performance than AWP applied in the latter layers. Furthermore, AWP applied to front layers reveals a positive robust generalization gap (training accuracy > testing accuracy) shortly after the first drop in learning rate, which continues to widen with further training. Conversely, AWP applied in the latter layers exhibits a negative robust generalization gap throughout most of the training, only converging to 0 after the second drop in learning rate. These differences demonstrate that worst-case perturbations, when injected into the latter layers' weights, have a more powerful impact in regularizing the optimization of AT. Consistent with our previous findings, AWP applied to the latter layers can be considered as an approach to regularize the optimization of AT in those layers, which successfully mitigates robust overfitting. This finding supports our analysis thus far, further demonstrating that regularizing the optimization of the latter layers is key to improving the robust generalization.

4 Experiment

In this section, we conduct extensive experiments to verify the effectiveness of RAT_{LR} and RAT_{WP}. Details of the experiment settings and performance evaluation are introduced below.

4.1 Experimental Setup

We conduct extensive experiments on two realizations of RAT under two threat models (L_∞ and L_2) across three benchmark datasets:

Table 1: Test robustness (%) on CIFAR10. We omit the standard deviations of 5 runs as they are very small ($< 0.6\%$).

Network	Threat Model	Method	PGD-20			AA		
			Best	Last	Diff	Best	Last	Diff
PreAct ResNet-18	L_∞	AT	52.31	44.45	7.86	47.95	42.05	5.90
		RAT_{LR}	51.57	49.07	2.50	46.89	45.35	1.54
		RAT_{WP}	**54.85**	**53.98**	**0.87**	**49.19**	**48.24**	**0.95**
	L_2	AT	69.27	65.86	3.41	67.65	64.64	3.01
		RAT_{LR}	68.97	68.21	**0.76**	64.26	63.44	**0.82**
		RAT_{WP}	**70.77**	**69.49**	1.28	**68.29**	**67.11**	1.18
Wide ResNet-34-10	L_∞	AT	55.57	47.37	8.20	52.13	46.09	6.04
		RAT_{LR}	55.50	47.32	8.18	52.05	45.89	6.16
		RAT_{WP}	**58.92**	**58.23**	**0.69**	**54.46**	**53.98**	**0.48**
	L_2	AT	70.57	68.99	**1.58**	69.44	66.92	**2.52**
		RAT_{LR}	**71.91**	68.94	2.96	**70.53**	**67.90**	2.63
		RAT_{WP}	71.31	**69.19**	2.12	70.12	67.35	2.77

Table 2: Test robustness (%) on CIFAR100. We omit the standard deviations of 5 runs as they are very small ($< 0.6\%$).

Network	Threat Model	Method	PGD-20			AA		
			Best	Last	Diff	Best	Last	Diff
PreAct ResNet-18	L_∞	AT	28.07	21.24	6.83	23.61	18.41	5.20
		RAT_{LR}	26.57	26.18	**0.39**	21.77	21.22	**0.55**
		RAT_{WP}	**30.91**	**30.42**	0.49	**25.52**	**24.57**	1.05
	L_2	AT	41.38	35.34	6.04	37.94	33.58	4.36
		RAT_{LR}	38.31	37.76	0.55	35.16	34.49	**0.77**
		RAT_{WP}	**45.23**	**44.93**	**0.3**	**41.32**	**39.47**	1.85
Wide ResNet-34-10	L_∞	AT	30.74	24.89	5.85	26.98	23.07	3.91
		RAT_{LR}	30.57	23.53	7.04	26.72	22.53	4.19
		RAT_{WP}	**30.81**	**25.46**	**5.35**	**27.11**	**23.56**	**3.55**
	L_2	AT	44.05	41.22	2.83	41.39	39.34	2.05
		RAT_{LR}	44.43	40.42	4.01	41.47	39.42	2.05
		RAT_{WP}	**46.12**	**44.64**	**1.48**	**41.94**	**40.38**	**1.56**

- CIFAR-10 (Krizhevsky et al., 2009). The CIFAR-10 dataset (Canadian Institute for Advanced Research, 10 classes) is a subset of the Tiny Images dataset and consists of 60000 32x32 color images. The images are labelled with one of 10 mutually exclusive classes: airplane, automobile (but not truck or pickup truck), bird, cat, deer, dog, frog, horse, ship, and truck (but not pickup truck). There are 6000 images per class with 5000 training and 1000 testing images per class.
- CIFAR-100 (Krizhevsky et al., 2009). The CIFAR-100 dataset (Canadian Institute for Advanced Research, 100 classes) is a subset of the Tiny Images dataset and consists of 60000 32x32 color images. The 100 classes in the CIFAR-100 are grouped into 20 superclasses. There are 600 images per class. Each image comes with a "fine" label (the class to which it belongs) and a "coarse" label (the superclass to which it belongs). There are 500 training images and 100 testing images per class.
- SVHN (Netzer et al., 2011). Street View House Numbers (SVHN) is a digit classification benchmark dataset that contains 600,000 32×32 RGB images of printed digits (from 0 to 9) cropped from pictures of house number plates. The cropped images are centered in the digit of interest, but nearby digits and other distractors are kept in the image. SVHN has three sets: training, testing sets and an extra set with 530,000 images that are less difficult and can be used for helping with the training process.

Table 3: Test robustness (%) on SVHN. We omit the standard deviations of 5 runs as they are very small ($< 0.6\%$).

Network	Threat Model	Method	PGD-20			AA		
			Best	Last	Diff	Best	Last	Diff
PreAct ResNet-18	L_∞	AT	53.10	44.12	8.98	45.09	40.36	**4.73**
		RAT_{LR}	53.32	43.41	9.92	45.98	39.61	6.37
		RAT_{WP}	**57.91**	**54.32**	**3.58**	**50.32**	**44.82**	5.49
	L_2	AT	66.29	64.73	**1.55**	63.55	**60.14**	**3.41**
		RAT_{LR}	66.47	62.10	4.36	62.44	58.72	3.72
		RAT_{WP}	**71.66**	**65.68**	5.98	**65.17**	59.64	5.53
Wide ResNet-34-10	L_∞	AT	55.57	47.11	8.46	48.05	42.46	5.59
		RAT_{LR}	55.34	46.81	8.53	47.94	42.12	5.82
		RAT_{WP}	**58.48**	**54.92**	**3.56**	**54.65**	**50.46**	**3.99**
	L_2	AT	67.19	**65.08**	**2.11**	62.58	**60.86**	**1.72**
		RAT_{LR}	67.50	64.24	3.27	62.79	59.94	2.85
		RAT_{WP}	**69.07**	64.76	4.31	**63.12**	59.57	3.55

Table 4: Performance (%) of RAT with other SOTA techniques on CIFAR-10 using PreAct ResNet-18 under L_∞ threat model ($\epsilon = 8/255$).

Method	PGD-20		
	Best	Last	Diff
AT	53.10	44.12	8.98
AWP	55.39	**54.73**	0.66
SWA	52.14	51.53	**0.61**
GAIRAT	**57.81**	53.76	4.05
RAT-LR	51.57	49.07	2.5
RAT-WP	54.85	53.98	0.87

We use PreAct ResNet-18 (He et al., 2016) and Wide ResNet-34-10 (Zagoruyko & Komodakis, 2016) following the same hyperparameter settings for AT in Rice et al. (2020): for L_∞ threat model, $\epsilon = 8/255$, step size is $1/255$ for SVHN, and $2/255$ for CIFAR-10 and CIFAR-100; for L_2 threat model, $\epsilon = 128/255$, step size is $15/255$ for all datasets. For training, all models are trained under 10-step PGD (PGD-10) attack for 200 epochs using SGD with momentum 0.9, weight decay 5×10^{-4}, and a piecewise learning rate schedule with an initial learning rate of 0.1. Standard data augmentation techniques, including random cropping with 4 pixels of padding and random horizontal flips, are applied. The models are decomposed into a series of 4 main layers, corresponding to 4 residual blocks of the ResNet architecture. For RAT_{LR}, learning rate for layer 3 & 4 are set to a fixed value of 0.1. For RAT_{WP}, weight perturbation is applied in layer 3 & 4, and other hyperparameters are configured as per the original paper. For testing, the robustness accuracy is evaluated under two different adversarial attacks, including 20-step PGD (PGD-20) and Auto Attack (AA) (Croce & Hein, 2020b). Auto Attack is considered the most reliable robustness evaluation to date, which is an ensemble of complementary attacks, consisting of three white-box attacks (APGD-CE (Croce & Hein, 2020b), APGD-DLR (Croce & Hein, 2020b), and FAB (Croce & Hein, 2020a)) and a black-box attack (Square Attack (Andriushchenko et al., 2020))

4.2 Performance Evaluation

In this section, we present the experimental results of RAT_{LR} and RAT_{WP} across three benchmark datasets.

CIFAR-10 Results. The evaluation results on CIFAR10 dataset are summarized in Table 1, where "Best" is the highest test robustness achieved during training; "Last" is the test robustness at the last epoch checkpoint; "Diff" denotes the robust accuracy gap between the "Best" & "Last". It is observed that RAT_{WP} generally achieves the best robust performance compared to RAT_{LR} & standard AT. Regardless, both RAT_{LR} and RAT_{WP} tighten the robustness gaps by a significant margin, indicating they can effectively suppress robust overfitting.

CIFAR-100 Results. We also show the results on CIFAR100 dataset in Table 2. We observe similar performance like CIFAR10, where both RAT_{LR} and RAT_{WP} is able to significantly reduce the robustness gaps. For robustness improvement, RAT_{WP} stands out to be the leading method. The results further verify the effectiveness of the proposed approach.

SVHN Results. The results on the SVHN dataset are shown in Table 3, where robustness gap are also narrowed down to a small margin by RAT_{WP}. SVHN dataset is a special case where RAT_{LR} strategy does not improve robust overfitting. Unlike CIFAR10 and CIFAR100, learning rate decay in SVHN's training does not have much connection to the sudden increases in robust test performance or the prevalence of robust overfitting, and hence makes RAT_{LR} ineffective. Other than this, The improvement in robust generalization gaps can be witnessed in all cases, demonstrating the proposed approachs are generic and can be applied widely.

Comparision with other SOTA methods. Finally, we provide the performance comparison with some of the existing SOTA methods under PreAct-ResNet18 architecture, L_∞ threat model and CIFAR-10 dataset in Table 4. These includes adversarial weight perturbation (Wu et al., 2020), learned smoothening (Chen et al., 2021b), instance reweighted (Zhang et al., 2020). In general, our methods are comparable to most of the SOTA methods, achieving adequate robustness with low degree of robust overfitting.

5 Conclusion

In this paper, we investigate the effects of different network layers on robust overfitting and identify that robust overfitting is mainly driven by the optimization occurred at the latter layers. Following this, we propose a *robust adversarial training* (RAT) prototype to specifically hinder the optimization of the latter layers in the process of training adversarial network. The approach prevents the model from overfitting the latter parts of the network, which effectively mitigate robust overfitting of the network as a whole. We then further demonstrate two implementations of RAT: one locally uses a fixed learning rate for the latter layers and the other utilize adversarial weight perturbation for the latter layers. Extensive experiments show the effectiveness of both approaches, suggesting RAT is generic and can be applied across different network architectures, threat models and benchmark datasets to solve robust overfitting.

References

Maksym Andriushchenko, Francesco Croce, Nicolas Flammarion, and Matthias Hein. Square attack: a query-efficient black-box adversarial attack via random search. In *European Conference on Computer Vision*, pp. 484–501. Springer, 2020.

Anish Athalye, Nicholas Carlini, and David Wagner. Obfuscated gradients give a false sense of security: Circumventing defenses to adversarial examples. In *International conference on machine learning*, pp. 274–283. PMLR, 2018.

Mikhail Belkin, Daniel Hsu, Siyuan Ma, and Soumik Mandal. Reconciling modern machine-learning practice and the classical bias–variance trade-off. *Proceedings of the National Academy of Sciences*, 116(32):15849–15854, 2019.

Yair Carmon, Aditi Raghunathan, Ludwig Schmidt, Percy Liang, and John C Duchi. Unlabeled data improves adversarial robustness. *arXiv preprint arXiv:1905.13736*, 2019.

Chen Chen, Jingfeng Zhang, Xilie Xu, Tianlei Hu, Gang Niu, Gang Chen, and Masashi Sugiyama. Guided interpolation for adversarial training. *arXiv preprint arXiv:2102.07327*, 2021a.

Tianlong Chen, Zhenyu Zhang, Sijia Liu, Shiyu Chang, and Zhangyang Wang. Robust overfitting may be mitigated by properly learned smoothening. In *International Conference on Learning Representations*, 2020.

Tianlong Chen, Zhenyu Zhang, Sijia Liu, Shiyu Chang, and Zhangyang Wang. Robust overfitting may be mitigated by properly learned smoothening. In *International Conference on Learning Representations*, 2021b.

Yunpeng Chen, Jianan Li, Huaxin Xiao, Xiaojie Jin, Shuicheng Yan, and Jiashi Feng. Dual path networks. *Advances in neural information processing systems*, 30, 2017.

Francesco Croce and Matthias Hein. Minimally distorted adversarial examples with a fast adaptive boundary attack. In *International Conference on Machine Learning*, pp. 2196–2205. PMLR, 2020a.

Francesco Croce and Matthias Hein. Reliable evaluation of adversarial robustness with an ensemble of diverse parameter-free attacks. In *International conference on machine learning*, pp. 2206–2216. PMLR, 2020b.

Jacob Devlin, Ming-Wei Chang, Kenton Lee, and Kristina Toutanova. Bert: Pre-training of deep bidirectional transformers for language understanding. *arXiv preprint arXiv:1810.04805*, 2018.

Chengyu Dong, Liyuan Liu, and Jingbo Shang. Label noise in adversarial training: A novel perspective to study robust overfitting. *Advances in Neural Information Processing Systems*, 35:17556–17567, 2022a.

Yinpeng Dong, Ke Xu, Xiao Yang, Tianyu Pang, Zhijie Deng, Hang Su, and Jun Zhu. Exploring memorization in adversarial training. In *International Conference on Learning Representations*, 2022b.

Ian J Goodfellow, Jonathon Shlens, and Christian Szegedy. Explaining and harnessing adversarial examples. *arXiv preprint arXiv:1412.6572*, 2014.

Kaiming He, Xiangyu Zhang, Shaoqing Ren, and Jian Sun. Deep residual learning for image recognition. In *Proceedings of the IEEE conference on computer vision and pattern recognition*, pp. 770–778, 2016.

Alex Krizhevsky, Geoffrey Hinton, et al. Learning multiple layers of features from tiny images. 2009.

Saehyung Lee, Hyungyu Lee, and Sungroh Yoon. Adversarial vertex mixup: Toward better adversarially robust generalization. In *Proceedings of the IEEE/CVF Conference on Computer Vision and Pattern Recognition*, pp. 272–281, 2020.

Lin Li and Michael Spratling. Data augmentation alone can improve adversarial training. *arXiv preprint arXiv:2301.09879*, 2023.

Fangzhou Liao, Ming Liang, Yinpeng Dong, Tianyu Pang, Xiaolin Hu, and Jun Zhu. Defense against adversarial attacks using high-level representation guided denoiser. In *Proceedings of the IEEE Conference on Computer Vision and Pattern Recognition*, pp. 1778–1787, 2018.

Feng Liu, Bo Han, Tongliang Liu, Chen Gong, Gang Niu, Mingyuan Zhou, Masashi Sugiyama, et al. Probabilistic margins for instance reweighting in adversarial training. *Advances in Neural Information Processing Systems*, 34:23258–23269, 2021.

Aleksander Madry, Aleksandar Makelov, Ludwig Schmidt, Dimitris Tsipras, and Adrian Vladu. Towards deep learning models resistant to adversarial attacks. *arXiv preprint arXiv:1706.06083*, 2017.

Amir Najafi, Shin-ichi Maeda, Masanori Koyama, and Takeru Miyato. Robustness to adversarial perturbations in learning from incomplete data. *Advances in Neural Information Processing Systems*, 32, 2019.

Preetum Nakkiran, Gal Kaplun, Yamini Bansal, Tristan Yang, Boaz Barak, and Ilya Sutskever. Deep double descent: Where bigger models and more data hurt. In *International Conference on Learning Representations*, 2020. URL `https://openreview.net/forum?id=B1g5sA4twr`.

Yuval Netzer, Tao Wang, Adam Coates, Alessandro Bissacco, Bo Wu, and Andrew Y Ng. Reading digits in natural images with unsupervised feature learning. 2011.

Nicolas Papernot, Patrick McDaniel, Xi Wu, Somesh Jha, and Ananthram Swami. Distillation as a defense to adversarial perturbations against deep neural networks. In *2016 IEEE symposium on security and privacy (SP)*, pp. 582–597. IEEE, 2016.

Sylvestre-Alvise Rebuffi, Sven Gowal, Dan Andrei Calian, Florian Stimberg, Olivia Wiles, and Timothy A Mann. Data augmentation can improve robustness. *Advances in Neural Information Processing Systems*, 34:29935–29948, 2021.

Leslie Rice, Eric Wong, and Zico Kolter. Overfitting in adversarially robust deep learning. In *International Conference on Machine Learning*, pp. 8093–8104. PMLR, 2020.

Ludwig Schmidt, Shibani Santurkar, Dimitris Tsipras, Kunal Talwar, and Aleksander Madry. Adversarially robust generalization requires more data. *Advances in neural information processing systems*, 31, 2018.

Karen Simonyan and Andrew Zisserman. Very deep convolutional networks for large-scale image recognition. *arXiv preprint arXiv:1409.1556*, 2014.

Chubiao Song, Kun He, Jiadong Lin, Liwei Wang, and John E Hopcroft. Robust local features for improving the generalization of adversarial training. In *International Conference on Learning Representations*, 2020.

Christian Szegedy, Wojciech Zaremba, Ilya Sutskever, Joan Bruna, Dumitru Erhan, Ian Goodfellow, and Rob Fergus. Intriguing properties of neural networks. *arXiv preprint arXiv:1312.6199*, 2013.

Florian Tramèr, Alexey Kurakin, Nicolas Papernot, Ian Goodfellow, Dan Boneh, and Patrick McDaniel. Ensemble adversarial training: Attacks and defenses. In *International Conference on Learning Representations*, 2018.

Jonathan Uesato, Jean-Baptiste Alayrac, Po-Sen Huang, Robert Stanforth, Alhussein Fawzi, and Pushmeet Kohli. Are labels required for improving adversarial robustness? *arXiv preprint arXiv:1905.13725*, 2019.

Yifei Wang, Liangchen Li, Jiansheng Yang, Zhouchen Lin, and Yisen Wang. Balance, imbalance, and rebalance: Understanding robust overfitting from a minimax game perspective. In *Thirty-seventh Conference on Neural Information Processing Systems*, 2023.

Yisen Wang, Difan Zou, Jinfeng Yi, James Bailey, Xingjun Ma, and Quanquan Gu. Improving adversarial robustness requires revisiting misclassified examples. In *International Conference on Learning Representations*, 2019.

Dongxian Wu, Shu-Tao Xia, and Yisen Wang. Adversarial weight perturbation helps robust generalization. *arXiv preprint arXiv:2004.05884*, 2020.

Jason Yosinski, Jeff Clune, Yoshua Bengio, and Hod Lipson. How transferable are features in deep neural networks? *Advances in neural information processing systems*, 27, 2014.

Chaojian Yu, Bo Han, Li Shen, Jun Yu, Chen Gong, Mingming Gong, and Tongliang Liu. Understanding robust overfitting of adversarial training and beyond. In *International Conference on Machine Learning*, pp. 25595–25610. PMLR, 2022.

Fisher Yu, Dequan Wang, Evan Shelhamer, and Trevor Darrell. Deep layer aggregation. In *Proceedings of the IEEE conference on computer vision and pattern recognition*, pp. 2403–2412, 2018.

Sergey Zagoruyko and Nikos Komodakis. Wide residual networks. In *British Machine Vision Conference 2016*. British Machine Vision Association, 2016.

Runtian Zhai, Tianle Cai, Di He, Chen Dan, Kun He, John Hopcroft, and Liwei Wang. Adversarially robust generalization just requires more unlabeled data. *arXiv preprint arXiv:1906.00555*, 2019.

Hongyang Zhang, Yaodong Yu, Jiantao Jiao, Eric Xing, Laurent El Ghaoui, and Michael Jordan. Theoretically principled trade-off between robustness and accuracy. In *International Conference on Machine Learning*, pp. 7472–7482. PMLR, 2019.

Jingfeng Zhang, Jianing Zhu, Gang Niu, Bo Han, Masashi Sugiyama, and Mohan Kankanhalli. Geometry-aware instance-reweighted adversarial training. *arXiv preprint arXiv:2010.01736*, 2020.

A More Evidences on the Layer-wise Properties of Robust Overfitting

In this section, we provide more empirical experiments to showcase the layer-wise properties of robust overfitting across different datasets, network architectures, threat models and adversarial training methods. Specifically, we use the proposed strategies mentioned in Section 3.3 to put restriction on the optimization of different network layers. We can always observe that there is significant robust overfitting relief when we regularize the optimization of the latter layers, while robust overfitting is prevalent for other settings. These evidences further highlight the strong relation between robust overfitting and the optimization of the latter layers.

A.1 Evidences across datasets

We show that the layer-wise properties of robust overfitting are universal across datasets on CIFAR-100 and SVHN. We adversarially train PreAct ResNet-18 using AT under l_∞ threat model on different datasets with the same settings as Section 3.3. The results are shown in Figure 5 and 6. Note that for SVHN, regularization strategy utilizing a fixed learning rate (RAT_{LR}) does not improve robust overfitting (Figure 5). Unlike CIFAR10 and CIFAR100, SVHN's robust overfitting appears before the first learning rate decay. Also, learning rate decay in SVHN's training does not have any relation to the sudden increases in robust test performance or the appearance of robust overfitting. Hence, SVHN dataset is a special case where RAT_{LR} does not apply. For all other cases, robust overfitting is effectively mitigated by regularizing the optimization of the latter layers.

A.2 Evidences across threat models

We further demonstrate that the generality of layer-wise properties of robust overfitting by conducting experiments under l_2 threat model. The settings are the same as Section 3.3. The results are shown in Figure 7 and 8. Under l_2 threat model, except for SVHN dataset where regularization strategy utilizing a fixed learning rate (RAT_{LR}) does not apply, robust overfitting is effectively mitigated by regularizing the optimization of the latter layers.

A.3 Evidences across network architectures

In this part, we show that the generality of layer-wise properties of robust overfitting by conducting experiments across different network architectures (PreAct ResNet-18 (He et al., 2016), PreAct ResNet-34 (He et al., 2016), VGG-16 (Simonyan & Zisserman, 2014), DPN-26 (Chen et al., 2017) and DLA (Yu et al., 2018)). For PreAct ResNet-18 and PreAct ResNet-34, the division of the network layer are the same as Section 3.3. For DPN-26 and DLA, similarly, we consider the four main network blocks separately for layer1, layer2, layer3 and layer4. For VGG-16, "features.0", "features.1", "features.3", "features.4", "features. 7", "features.8" are regarded as layer1, "features.10", "features.11", "features.14", "features.15", "features .17", "features.18" are regarded as layer2, "features.20", "features.21", "features.24", "features.25 ", "features.27", "features.28", "features.30" are regarded as layer3, and "features.31", "features.34' ', "features.35", "features.37", "features.38", "features.40", "features.41" are regarded as layer4. The results are shown in Figure 9. These results clearly indicate that the optimization of the latter layers present a strong correlation to the robust overfitting phenomenon, and the layer-wise properties of robust overfitting are common in different network architectures.

A.4 Evidences across adversarial training methods

We further demonstrate that the generality of layer-wise properties of robust overfitting by conducting experiments using different adversarial training methods (Standard AT (Madry et al., 2017) and TRADES

(Zhang et al., 2019)). The settings are the same as Section 3.3. The results are shown in Figure 10. The experiments results indicate that the latter layers have stronger connections to robust overfitting than the front layers do, and the layer-wise properties of robust overfitting is generally hold regardless of the chosen adversarial training methods.

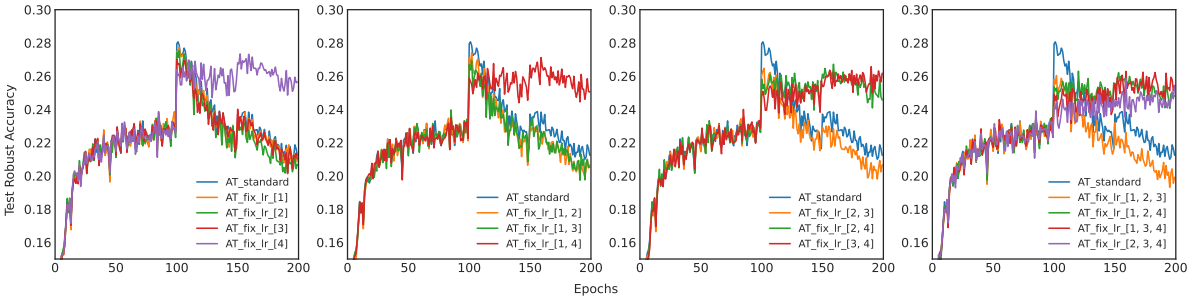

(a) AT using PreAct ResNet-18 on CIFAR100 dataset under l_∞ threat model

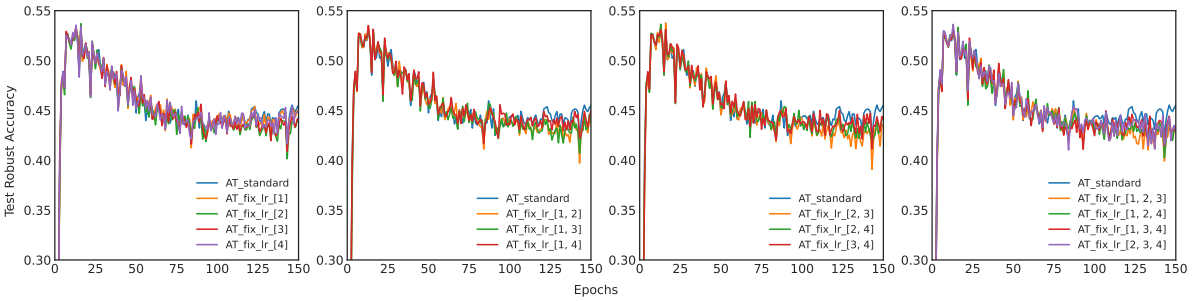

(b) AT using PreAct ResNet-18 on SVHN dataset under l_∞ threat model

Figure 5: Robust test performance of AT using a fixed learning rate for different sets of network layers in PreAct ResNet-18, across datasets (CIFAR-100 and SVHN) under l_∞ threat model.

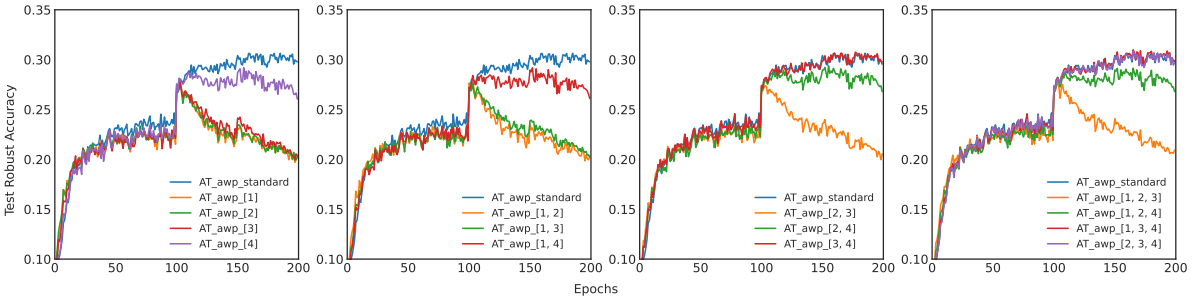

(a) AT using PreAct ResNet-18 on CIFAR100 dataset under l_∞ threat model

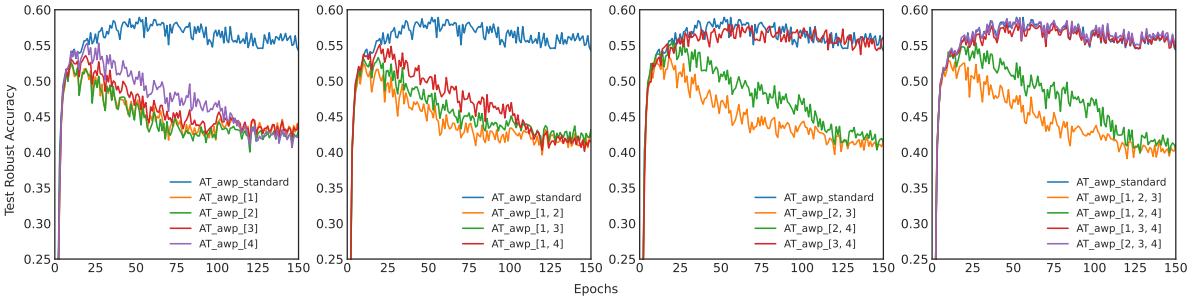

(b) AT using PreAct ResNet-18 on SVHN dataset under l_∞ threat model

Figure 6: Robust test performance of AT applying AWP for different sets of network layers in PreAct ResNet-18, across datasets (CIFAR-100 and SVHN) under l_∞ threat model.

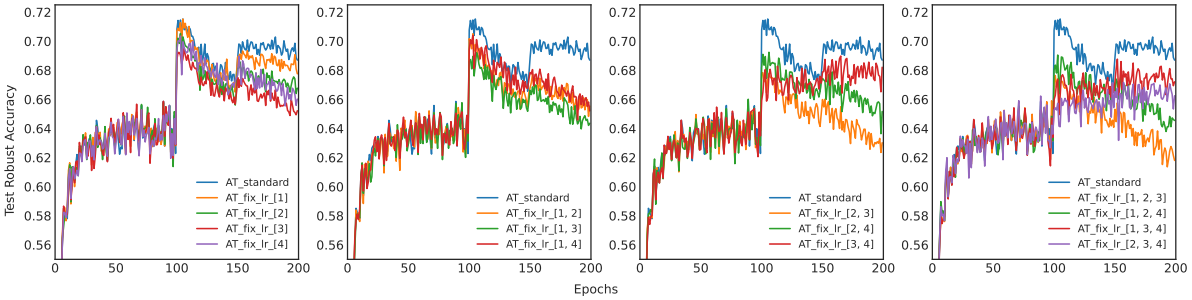

(a) AT using PreAct ResNet-18 on CIFAR10 dataset under l_2 threat model

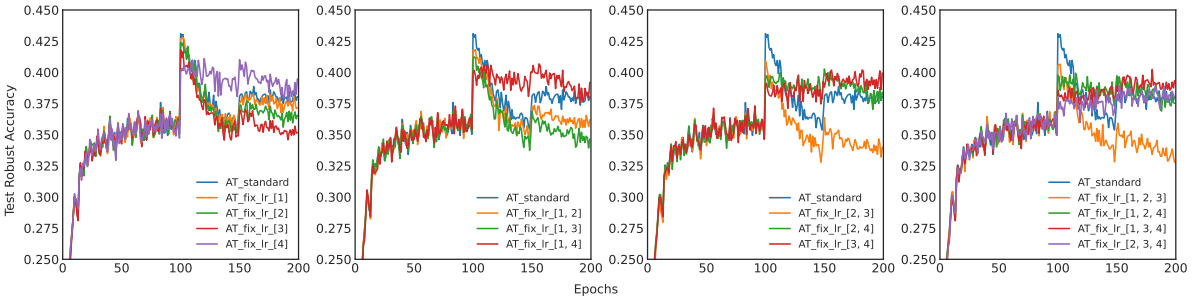

(b) AT using PreAct ResNet-18 on CIFAR100 dataset under l_2 threat model

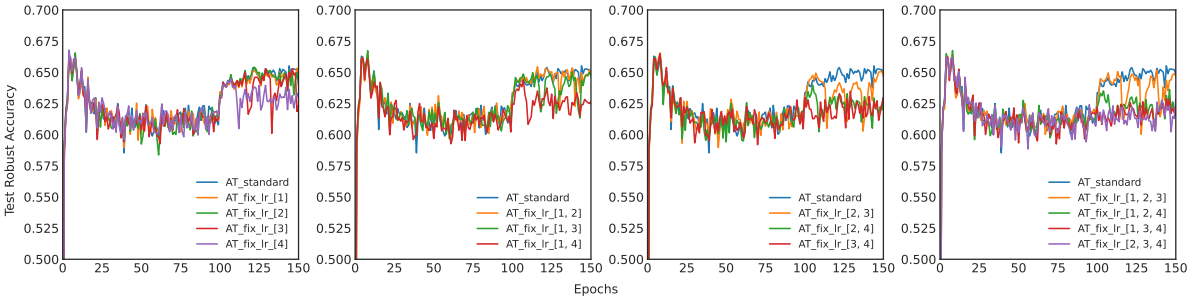

(c) AT using PreAct ResNet-18 on SVHN dataset under l_2 threat model

Figure 7: Robust test performance of AT using a fixed learning rate for different sets of network layers in PreAct ResNet-18, across datasets (CIFAR-10, CIFAR-100 and SVHN) under l_2 threat model.

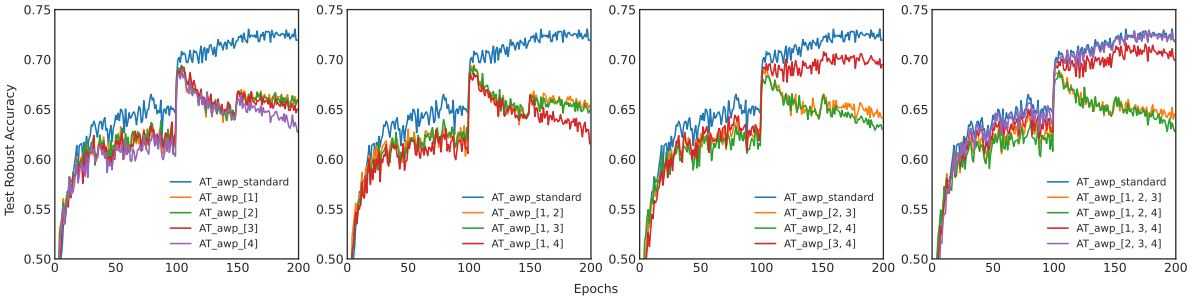

(a) AT using PreAct ResNet-18 on CIFAR10 dataset under l_2 threat model

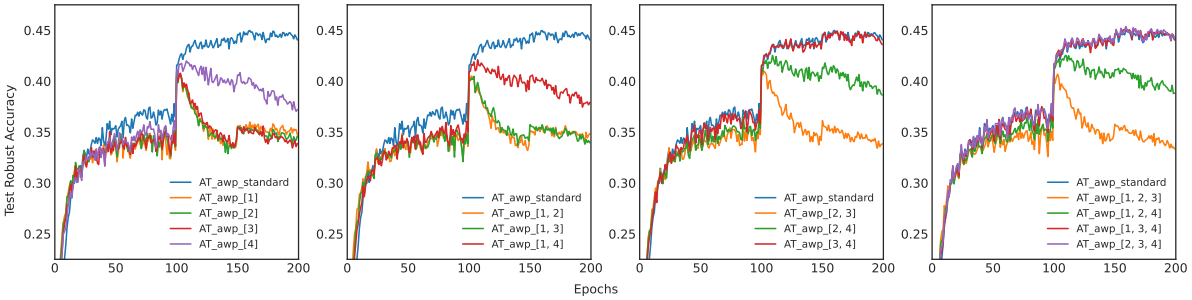

(b) AT using PreAct ResNet-18 on CIFAR100 dataset under l_2 threat model

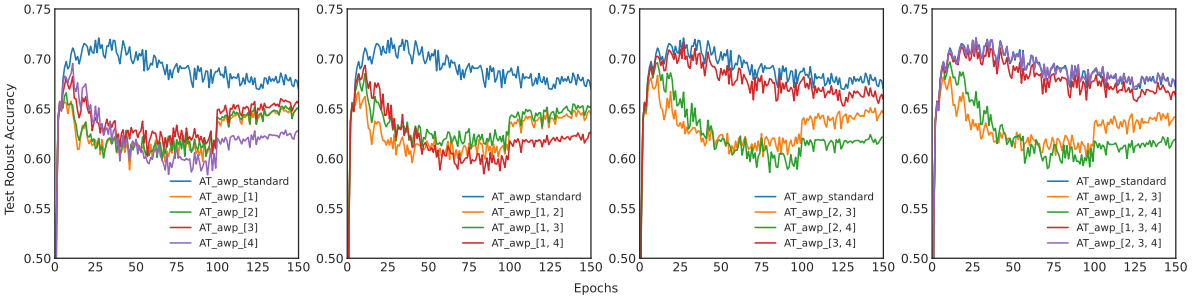

(c) AT using PreAct ResNet-18 on SVHN dataset under l_2 threat model

Figure 8: Robust test performance of AT applying AWP for different sets of network layers in PreAct ResNet-18, across datasets (CIFAR10, CIFAR-100 and SVHN) under l_2 threat model.

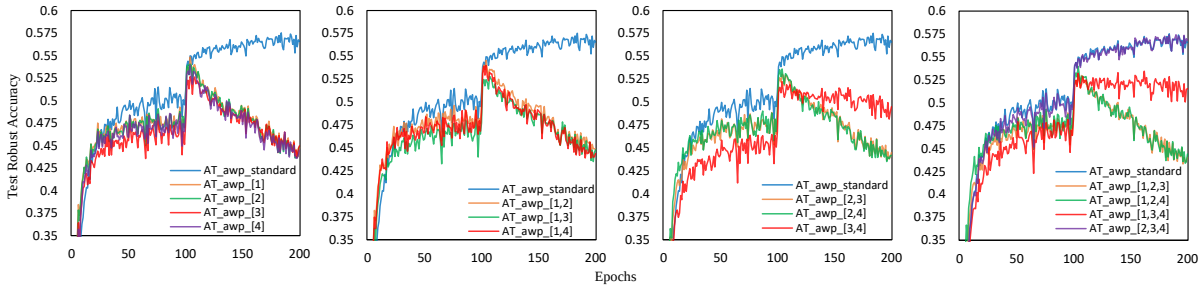

(a) AT using PreAct ResNet-34 on CIFAR10 dataset under l_∞ threat model

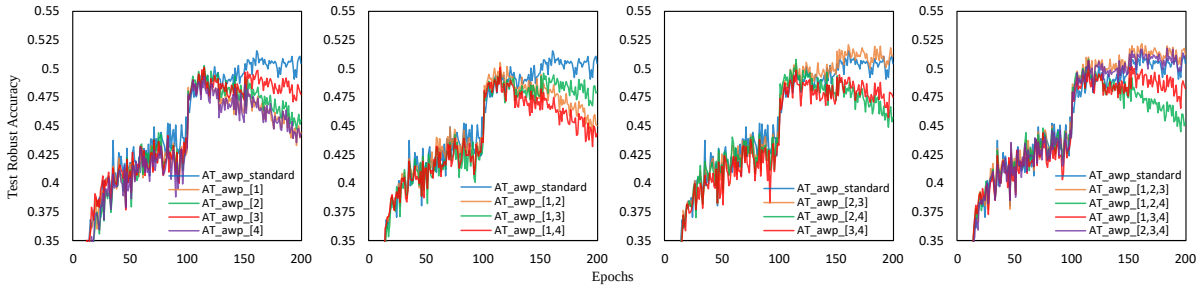

(b) AT using VGG-16 on CIFAR10 dataset under l_∞ threat model

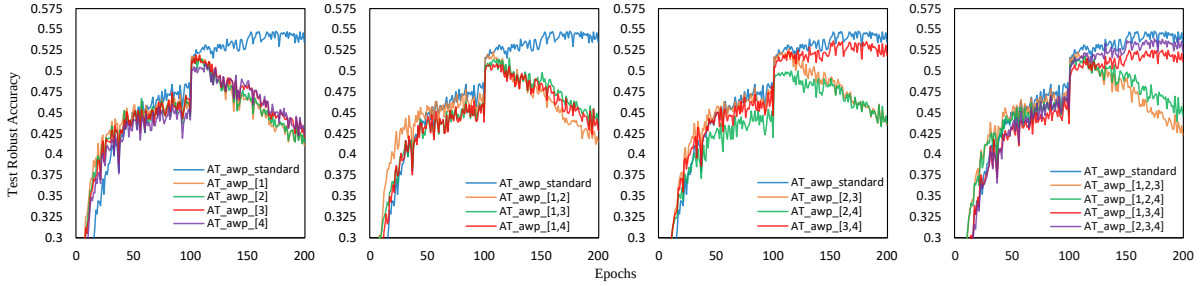

(c) AT using DPN-26 on CIFAR10 dataset under l_∞ threat model

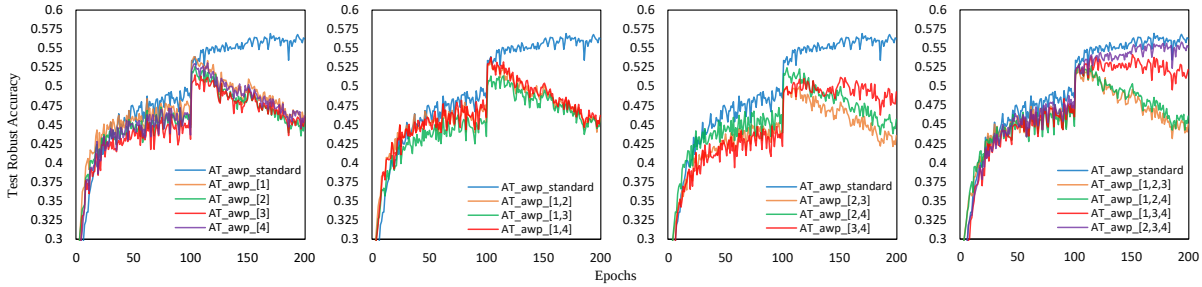

(d) AT using DLA on CIFAR10 dataset under l_∞ threat model

Figure 9: Robust test performance of AT applying AWP for different sets of network layers across network architectures (PreAct ResNet-34, VGG-16, DPN-26 and DLA), on CIFAR-10 datasets under l_∞ threat model.

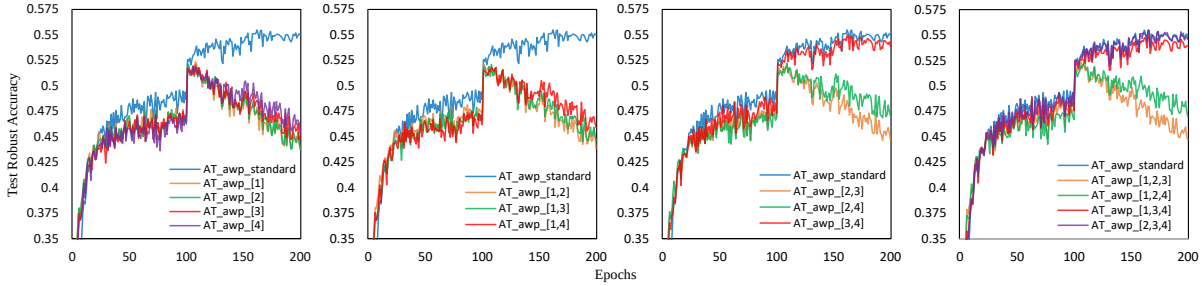

(a) AT using PreAct ResNet-18 on CIFAR10 dataset under l_∞ threat model

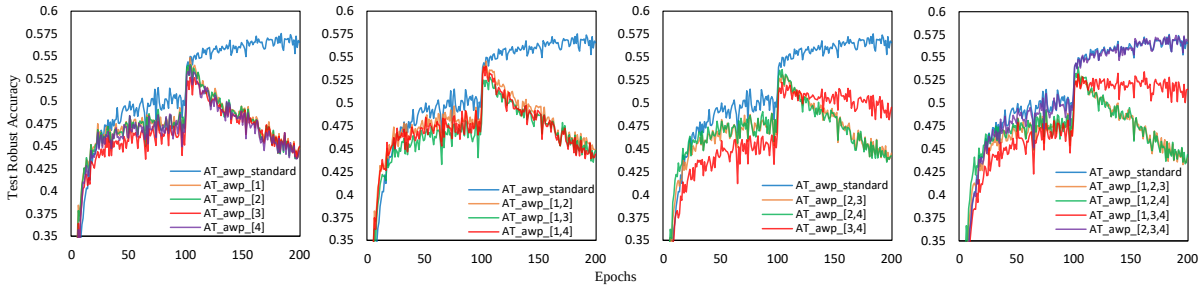

(b) AT using PreAct ResNet-34 on CIFAR10 dataset under l_∞ threat model

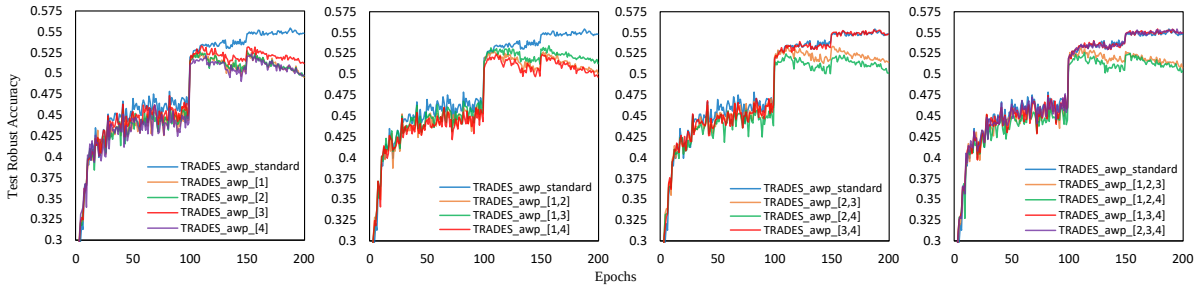

(c) TRADES using PreAct ResNet-18 on CIFAR10 dataset under l_∞ threat model

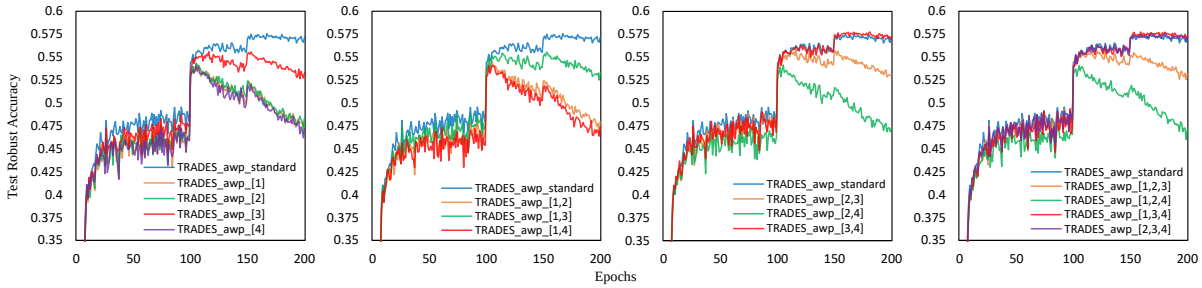

(d) TRADES using PreAct ResNet-34 on CIFAR10 dataset under l_∞ threat model

Figure 10: Robust test performance of AT and TRADES applying AWP for different sets of network layers in PreAct ResNet-18 and PreAct ResNet-34, on CIFAR-10 datasets under l_∞ threat model.